Modeling of the rough-interface effect on a converging light beam propagating in a skin tissue phantom

Jun Q. Lu, Xin-Hua Hu, and Ke Dong

Light distribution in a strong turbid medium such as skin tissue depends on both the bulk optical properties and the profiles of the interfaces where mismatch in the refractive index occurs. We present recent results of a numerical investigation on the light distribution inside a human skin tissue phantom for a converging laser beam with a wavelength near 1 μm and its dependence on the roughness of the interfaces and index mismatch. The skin tissue is modeled by a two-layer structure, and within each layer the tissue is considered macroscopically homogeneous. The two interfaces that separate the epidermis from the ambient medium and the dermis are considered randomly rough. With a recently developed method of Monte Carlo simulation capable of treating inhomogeneous boundary conditions, light distributions in various cases of interface roughness and index mismatch are obtained, and their relevance to the measurements of optical parameters of the skin tissue and laser surgery under the skin surface are discussed.

OCIS codes: 170.0170, 240.5770, 170.6930, 170.1870.

1. Introduction

Accurate understanding of the optical properties of human skin remains a challenge to biomedical optics,[1,2] and theoretical modeling of light propagation in skin tissues continues to be active. The radiative transfer theory has served as a major framework of modeling light propagation and distribution within which various numerical approaches have been pursued because analytical solutions are rarely feasible.[3] Among these approaches, the Monte Carlo simulation, in which a model of independent photons undergoing random walk is used, has acquired considerable preference over others for its strong capability to provide nearly exact solutions with simple algorithms in spite of the intense computing requirement.[4–7] The effect of skin tissue structure on light distribution has been previously investigated through various layer models in which optically smooth interfaces were assumed between the layers, and therefore only bulk scattering has been considered in descriptions of the propagation of collimated laser beams in skin tissue phantoms.[8–10] It is well known, however, that the skin layer interfaces are inherently rough, and it is desirable that the interface roughness be taken into consideration for quantitative understanding of its effect on light distribution. Possible benefits of this knowledge include improving accuracy in determination of the tissue optical parameters, clarifying understanding of the tissue structure through confocal imaging and optical coherent tomography,[11,12] and gaining insight into developing new methods to treat various lesions in a skin dermal layer with focused laser beams.[13] In pursuing this goal we have recently developed a method of Monte Carlo simulation that is capable of directly calculating the light distribution inside a turbid medium for light beams of any configuration and tissue interfaces of arbitrary profiles.[14] With this method the incident beam is treated as a collection of independent photons, and each photon is individually tracked according to the boundary condition and phantom geometry within the framework of radiative transfer theory. The computation efficiency of this method is obtained through a time-slicing procedure by exploitation of the linear relation between the photon pathlength and its travel time for the spatial distribution of photon density.[14] In this paper we present simulation results of light distribution in a two-layer model of human skin tissue with rough interfaces for a con-

The authors are with the Department of Physics, East Carolina University, Greenville, North Carolina 27858. J. Q. Lu's e-mail address is luj@mail.ecu.edu.

Received 20 April 2000; revised manuscript received 27 June 2000.

0003-6935/00/315890-08$15.00/0

verging light beam and discuss implications of these results. The photons in the incident beam are coupled into this two-layer tissue phantom, and their propagation directions may be altered at incidence upon an interface because of variations in the local slope of the interface. Additionally, the photons will experience random scattering and absorption because of microscopic fluctuations in the refractive index and various chromophores in the skin tissue.

2. Skin Modeling

Skin is considered the largest and heaviest organ of the human body, and its superficial structure is composed of two primary layers: the epidermis and the underlying dermis.[15] The epidermis consists of keratinizing sublayers supported by the dermal layer of dense fibroelastic connective tissues containing glands and hairs. The average thickness of the dermis is ~3 mm whereas that of the epidermis is between 50 and 150 μm. As the most superficial layer of the skin, the epidermis can be divided further into five sublayers, within which the structure of the outermost sublayer determines the roughness of the skin surface. The principal cells of the epidermis are keratinocytes, which gradually migrate from the deepest stratum to the surface and are sloughed off in a process called desquamation. The cornified and outermost sublayer of the epidermis is the stratum corneum, which has a thickness of approximately 6 μm. The stratum corneum contains some 15 layers of flattened, nonnucleated, keratinized cells called corneocytes, which are filled with filaments of keratin. The disk-shaped corneocyte cells with large cross sections are dehydrated with a thickness of 0.2–0.4 μm in the direction perpendicular to the skin surface.[16] Because the corneocytes are arranged in vertical columns that resemble stacks of flat disks, the microscopic fluctuation of the skin surface height is expected to be approximately the cell thickness. The corneocytes have lateral diameters of approximately 30 μm in the plane of the skin surface, or the x–y plane, with edges overlapped.[16] Assuming that the microscopic structure of the skin surface on the scale of micrometers is determined by the top layer of corneocytes, we expect that the average vertical peak–valley distances lie in the neighborhood of 0.3 μm over a lateral distance of 20 μm in the x–y plane, parallel to the skin surface. The relatively large structures of the human skin surface, such as the glyphic patterns and wrinkles, have linear sizes ranging from a fraction of 1 mm to a few millimeters. These structures vary considerably according to the skin region and are influenced by age and skin diseases. In fact, the glyphic lines disappear in the scalp and the tip of the nose.[17] Because the linear sizes of these surface structures are similar to or larger than the diameter of the converging beam considered in our simulations, their effect on deflecting light penetrating into skin is less significant than that of the microscopic structures and thus will not be considered in our model.

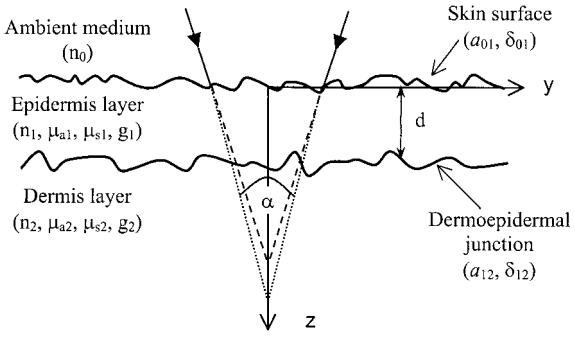

Fig. 1. Schematic drawing of the two-layer model for human skin tissue, with a converging laser beam of cone angle α incident upon the surface. All simulation results were obtained assuming a laser beam of Gaussian profile with $\alpha = 30°$ and the average thickness of the epidermis $d = 60$ μm.

We adopt a two-layer model of the human skin that is sufficient for our considerations of light distribution in the upper dermis within 2 mm from the skin surface. In our two-layer model, the epidermis layers are treated as infinite slabs in the transverse x–y plane with an average thickness d along the z axis, whereas the dermis is treated as a semi-infinite medium below the dermoepidermal junction, as shown in Fig. 1. Each layer is assumed to be macroscopically homogeneous and has its own set of optical parameters: refractive index n_i, absorption coefficient μ_{ai}, scattering coefficient μ_{si}, and mean cosine of the scattering angle or the anisotropy factor g_i, with $i = 1$ for the epidermis and $i = 2$ for the dermis. The dominant absorber of the near-infrared laser radiation at wavelengths near 1 μm in the epidermis is melanin, and we choose $\mu_{a1} = 5.0\ \text{mm}^{-1}$, with $\mu_{s1} = 10.0\ \text{mm}^{-1}$ and $g_1 = 0.9$ (Refs. 2 and 6). In the dermal layer the principal absorber is hemoglobin, which absorbs the near-infrared light near 1 μm weakly. Therefore the bulk absorption coefficient of the dermis is chosen to be smaller than that of the epidermis: $\mu_{a2} = 0.5\ \text{mm}^{-1}$, with $\mu_{s2} = 5.0\ \text{mm}^{-1}$ and $g_2 = 0.9$.[7]

3. Rough Interface

In our two-layer skin model shown in Fig. 1, the two interfaces separating the skin epidermis from the ambient medium and the dermis are assumed to have height fluctuation and are modeled as two-dimensional random rough surfaces in the x–y plane. A statistical technique widely used in the scattering of electromagnetic waves from random rough surfaces[18–20] is employed to generate the random surfaces numerically. Here each interface is described by a surface-profile function, with the interface between the ambient medium and the epidermis described by $z = \zeta_1(\mathbf{R})$ and the interface between the epidermis and the dermis by $z = d + \zeta_2(\mathbf{R})$, where $\mathbf{R} = (x, y)$ is the position vector in the xy plane and d is the mean thickness of the epidermis layer. The profile functions $\zeta_1(\mathbf{R})$ and $\zeta_2(\mathbf{R})$ are statistically independent, and each is assumed to be a stationary

Gaussian stochastic process characterized by a zero mean and Gaussian surface-height correlation function, as expressed in the following equations:

$$\langle \zeta_i(\mathbf{R}) \rangle = 0, \tag{1}$$

$$\langle \zeta_i(\mathbf{R}) \zeta_i(\mathbf{R}') \rangle = \delta_i^2 \exp[-(\mathbf{R} - \mathbf{R}')^2 / a_i^2], \tag{2}$$

where $i = 1, 2$ for the first (at $z = 0$) and the second (at $z = d$) interfaces, respectively. The parameter δ_i is the rms height of the surface departure from flatness, describing the vertical fluctuation; the parameter a is the transverse correlation length of the surface roughness, describing the average lateral distance between the peak and the valley in the surface profile. The angle brackets denote an average over the ensemble of realizations of surface profile. Numerically, each profile function in the ensemble, say $\zeta(\mathbf{R})$, is generated from an uncorrelated Gaussian distribution of random numbers $X(\mathbf{R})$ through a convolution integration

$$\zeta(\mathbf{R}) = \frac{2\delta}{a\sqrt{\pi}} \int X(\mathbf{R}') \exp\left[-\frac{2(\mathbf{R} - \mathbf{R}')^2}{a^2} \right] d\mathbf{R}' \equiv X(\mathbf{R}) * G(\mathbf{R}), \tag{3}$$

where $X(\mathbf{R})$ is the random height at position $\mathbf{R}$ on the surface. To achieve a high computing efficiency, the profile function is obtained through fast Fourier transformations as

$$\zeta(\mathbf{R}) = \frac{1}{2\pi} \int x(\mathbf{Q}) g(\mathbf{Q}) \exp[i\mathbf{Q} \cdot \mathbf{R}] d\mathbf{Q}, \tag{4}$$

where $x(\mathbf{Q})$ and $g(\mathbf{Q})$ are the Fourier transformations of $X(\mathbf{R})$ and $G(\mathbf{R})$, respectively. In our Monte Carlo simulations, results from individual samples of a rough surface ensemble are averaged to yield the statistical distribution of light in the skin phantom.

Light reflection and refraction occur at an interface with mismatched refractive indices. When a beam of light is incident upon a rough interface separating two media of different refractive indices, the interaction of the electromagnetic field with the rough surface becomes complicated to analyze through the wave approach. In the limit that the wavelength of the incident light is much smaller than the transverse dimension of the roughness, we may approximate the incident electromagnetic field at any point of a rough surface by a field that would be presented on the plane tangential to the point, i.e., the Kirchhoff approximation.[21] Under this approximation the reflection and the refraction of light at a rough interface depend only on the local angle of incidence and refractive indices of the materials, and the Fresnel reflection coefficient can be invoked to determine the penetration of the light through the interface within the framework of radiative transfer theory.

From elementary geometrical considerations, the criterion for the Kirchhoff approximation to be valid is given by

$$4\pi R_c \cos \varphi_i \gg \lambda, \tag{5}$$

and that for use of the Fresnel coefficient[21]

$$(kR_c)^{1/3} \cos \varphi_i \gg 1, \tag{6}$$

where R_c is the radius of curvature of the surface, φ_i is the angle of incidence measured against the local surface normal, and $k = 2\pi/\lambda$. In the present case the wavelength is $\lambda \sim 1$ μm, and both R_c and φ_i can be estimated from their mean values based on the surface roughness parameters a and δ. R_c can be estimated from the formula for the rms curvature of a random grating surface,[22] $R_c = (a^2/\delta)(2\sqrt{3})$; φ_i can be estimated by calculation of the rms slope of a random surface,[19] $\langle \tan \varphi_i \rangle_{\text{rms}} = \langle \text{slope} \rangle_{\text{rms}} = \sqrt{2}\delta/a$. For the surface-roughness parameters used in this paper, $4\pi R_c \langle \cos \varphi_i \rangle_{\text{rms}}$ is larger than 8×10^3 μm, and $(kR_c)^{1/3} \langle \cos \varphi_i \rangle_{\text{rms}}$ is larger than 16 for both interfaces; therefore both criteria (5) and (6) are satisfied completely. From these arguments, we thus treat the interfaces as locally flat and proceed to simulate light reflection and refraction at the rough interfaces through the calculation of the Fresnel reflection coefficient. The following algorithms are adopted to govern the light propagation when a rough interface is encountered.

Consider a photon arriving at a rough interface separating the incident medium of index n_i from the refractive medium of index n_r; the Fresnel reflection coefficient R at that point of the surface is calculated for the photon according to its local angle of incidence φ_i. To determine whether the photon is either reflected or refracted, a random number RND is selected from a uniform distribution between 0 and 1 and compared with R. The photon will be reflected if RND $< R$ or refracted into the other medium otherwise. If we designate unit vectors $\mathbf{i}$ for the direction of the incident photon, $\mathbf{r}$ for the direction of reflection, $\mathbf{t}$ for the direction of refraction, and $\mathbf{n}$ for the direction of the local surface normal pointing in the direction of the z axis, the following relations among the unit vectors can be obtained:

$$\mathbf{r} = 2(\cos \varphi_i)\mathbf{n} + \mathbf{i}, \tag{7}$$

$$\mathbf{t} = \frac{\sin(\varphi_r - \varphi_i)}{\sin \varphi_i} \mathbf{n} + \frac{n_i}{n_r} \mathbf{i}. \tag{8}$$

These provide the direction of propagation of the photon after its encounter with the interface. Figure 2 illustrates the geometrical relations. In Eqs. (7) and (8) the refraction angle φ_r is related to the incident angle φ_i by Snell's law: $n_i \sin \varphi_i = n_r \sin \varphi_r$, and φ_i is given by $\cos \varphi_i = \mathbf{i} \cdot \mathbf{n}$. For a rough interface with a given profile function $\zeta(\mathbf{R})$, $\mathbf{n}$ is calculated from the

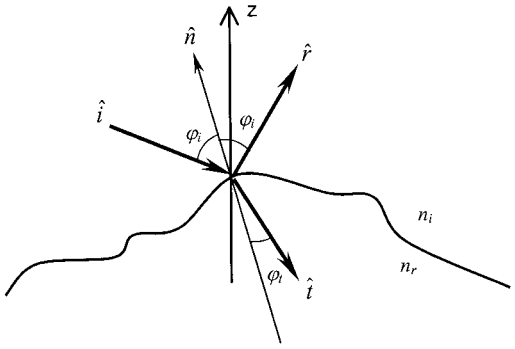

Fig. 2. Geometric relations among the various unit vectors at an interface between two media of different refractive index n_i and n_r.

partial derivatives of the profile function, ζ_x' and ζ_y', at the point of incidence:

$$\mathbf{n} = \frac{-\zeta_x'\mathbf{x} - \zeta_y'\mathbf{y} + \mathbf{z}}{(\zeta_x'^2 + \zeta_y'^2 + 1)^{1/2}}, \tag{9}$$

where $\mathbf{x}$, $\mathbf{y}$, and $\mathbf{z}$ are the unit vectors along the respective axes.

The coefficient R is calculated from φ_i, n_i, and n_r based on Fresnel's formula, averaged in both s and p polarization because the light within the radiative transfer theory is treated as photons without polarization:

$$R = \frac{1}{2}\left\{\left[\frac{\tan(\varphi_i - \varphi_r)}{\tan(\varphi_i + \varphi_r)}\right]^2 + \left[\frac{\sin(\varphi_i - \varphi_r)}{\sin(\varphi_i + \varphi_r)}\right]^2\right\} \quad \text{for } \varphi_i > 0, \tag{10}$$

where R reduces to $R = [(n_r - n_i)/(n_r + n_i)]^2$ for $\varphi_i = 0$.

4. Results

We simulate the propagation of a converging laser beam in the two-layer skin model because this type of beam configuration is of interest for a wide range of imaging and therapeutic applications of lasers. The time-slicing Monte Carlo method reported recently[14] is used to calculate the light distribution in the tissue. The mean thickness of the epidermis layer d is set to be 60 μm. The converging laser beam is assumed to be of Gaussian profile and incident upon a tissue phantom, as shown in Fig. 1, with the beam axis on the z axis. The beam has a cone angle $\alpha = 30°$ in the ambient medium, and its radius at $z = 0$, or the mean level of the interface between the ambient medium and the tissue phantom, varies between 0.18 and 0.25 mm as the beam is shifted along the z axis to make the geometrical focal point fixed at $z = 1.0$ mm in the dermis layer for different indices of refraction for the ambient medium. Once the beam enters the tissue phantom, the undisturbed portion of the beam is assumed to proceed as a spherical wave toward the geometric focal point on the z axis without considering diffraction, consistent with radiative transfer theory. An ensemble of 60 realizations of the random rough surface is used for each of the two interfaces, and a total of 2.1×10^8 photons are tracked in each simulation to yield the light distribution in the skin tissue phantom. The parameters of the two rough interfaces and refractive indices of the two layers are varied to allow us to study the effect of interface roughness and index mismatch on light distribution.

The light reflection and refraction at an interface are results of the mismatch in the refractive index. Because of the complicated nature of skin tissue optics, no accurate database is available for the wavelength and tissue-type dependence of the index for human skin in the near-infrared region. To ensure the clinical relevance of our simulation results, we choose the skin refractive index from a range based on the existing literature to study the effect of index mismatch at rough interfaces. The refractive index of the skin dermis, n_2, is chosen to be in the neighborhood of 1.41 for our simulation for light with wavelengths near 1 μm (Ref. 12). The refractive index of the stratum corneum, consisting of dehydrated cells, has been cited[1,2] as 1.55. Because we consider mostly the cases of water as the ambient medium in contact with the stratum corneum, we assume the refractive index n_1 of the epidermis to be of two values between that of the water and the dehydrated stratum corneum: $n_1 = 1.41$ or $n_1 = 1.45$. Throughout the calculations, the bulk optical parameters are fixed at $\mu_{a1} = 5.0\ \text{mm}^{-1}$, $\mu_{s1} = 10.0\ \text{mm}^{-1}$, and $g_1 = 0.9$ for the epidermis layer and $\mu_{a2} = 0.5\ \text{mm}^{-1}$, $\mu_{s2} = 5.0\ \text{mm}^{-1}$, and $g_2 = 0.9$ for the dermis layer.[2,6,7] Also fixed in the calculations are the transverse correlation lengths, $a_{01} = 20$ μm and $a_{12} = 80$ μm, for the rough interfaces between the ambient medium and the epidermis and the dermoepidermal junction, respectively. The rms heights of the skin surface δ_{01} are varied from 0.1 to 0.4 μm, and the junction height δ_{12} from 10 to 20 μm based on a low-power micrograph of the vertical section of the human skin.[15]

We first investigate the effects of roughness solely at the skin surface on the light distribution inside tissue by setting the index of refraction to be the same for both epidermis and dermis layers, $n_1 = n_2 = 1.41$, and assuming air for the ambient medium ($n_0 = 1.0$). Shown in Fig. 3 is an example of simulated light distributions on the y–z plane inside the two-layer phantom of human skin tissue with $\delta_{01} = 0.2$ μm and $\delta_{12} = 20$ μm. Here we see a loosely focused beam of light with photon density decreasing as the beam propagates deeper into the tissue because of scattering and absorption in the medium. The dermoepidermal junction can be seen in the figure even for the matched index at the junction, since the two layers have different scattering and absorption coefficients. Because of the cylindrical symmetry of the problem, the distribution of the photon density along the z axis in the medium may be used to analyze the light distribution quantitatively in the two-layer model. The z dependence of the photon density corresponding to the case in Fig. 3 is plotted in Fig. 4 as the curve with

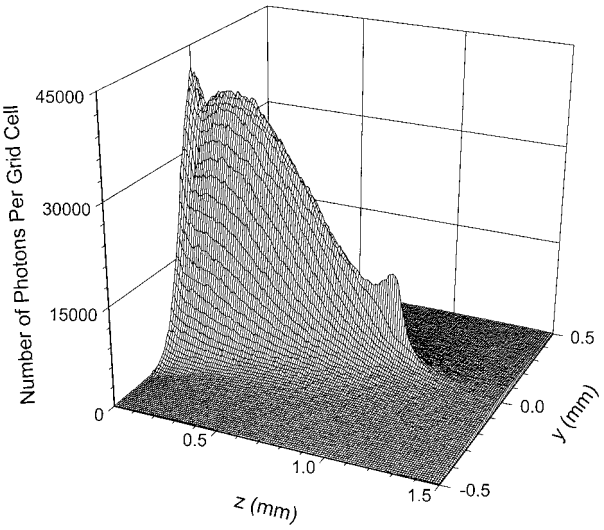

Fig. 3. Photon density in the y–z plane with air as the ambient medium ($n_0 = 1.00$) and the rms height at the skin surface δ_{01} set at 0.2 μm. The parameters of the two-layer skin tissue model are given by $n_1 = n_2 = 1.41$, $a_{01} = 20$ μm, $\mu_{a1} = 5.0$ mm^{-1}, $\mu_{s1} = 10.0$ mm^{-1}, $g_1 = g_2 = 0.9$, $a_{12} = 80$ μm, $\delta_{12} = 20$ μm, $\mu_{a2} = 0.5$ mm^{-1}, and $\mu_{s2} = 5.0$ mm^{-1}.

the lowest peak at the focal point located at $z = 1.0$ mm. It can be seen that the photon density decreases rapidly as the beam propagates in the epidermis layer, and when the beam enters the dermis layer the density first increases slowly and then starts to decrease as the beam penetrates deeper into the layer, and a local maximum appears at the focal point. The deeper decrease in density in the epidermis layer is due to the larger absorption coefficient μ_{a1} that is ~10 times that in the dermis layer (μ_{a2}). The initial slow increase in the density in the dermis layer is a combined result of the beam convergence and the relatively small scattering coefficient of the dermis layer. As the beam penetrates deeper into the layer, scattering events overwhelm the beam convergence that, enhanced by absorption, cause the decrease in the photon density. The local maximum observed at the focal point demonstrates the purpose of considering a converging beam, i.e., bringing all the undisturbed photons neither deflected at the interfaces because of the random nature of the local surface normal nor attenuated in the bulk together at the focal point. Similar peaks have been found and discussed in our previous study of various converging light beams propagating in a semi-infinite tissue phantom with a smooth and flat surface.[14] We can observe the effect of roughness at the skin surface clearly by comparing this curve with another one plotted in Fig. 4 in which the surface roughness is reduced to $\delta_{01} = 0.1$ μm. Compared with the previous case of $\delta_{01} = 0.2$ μm, nearly identical features of the density variation are observed, except that the peak at the focal point is much higher in the present case. This quantitatively shows that the surface roughness significantly affects the distribution of only those undisturbed photons arriving near the focal spot.

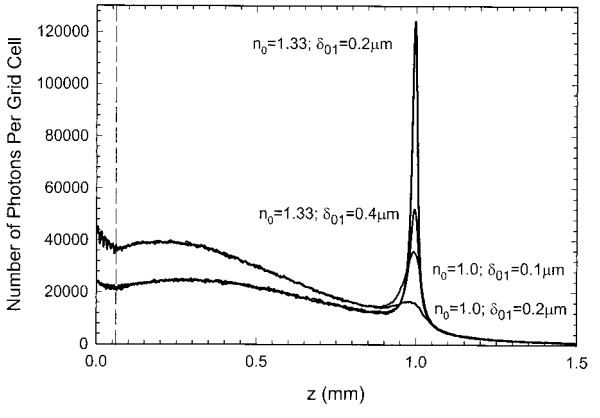

Fig. 4. Photon density z dependence on the z axis. Results from four simulation cases are displayed with different indices of the ambient medium n_0 and the rms height at the skin surface δ_{01}. All other parameters remain the same as those in Fig. 3, and the dashed line indicates the position of the dermoepidermal junction.

The effect of the index mismatch at the skin surface is displayed in Fig. 4, with air ($n_0 = 1.0$) replaced with water ($n_0 = 1.33$) as the ambient medium. A reduced mismatch at the skin surface leads to a much stronger peak at the focal point for the same rough interface shown in Fig. 3. When the air is replaced with water as the ambient medium, the beam radius at the skin surface is increased from 0.188 to 0.252 mm in the simulations to keep the focal point fixed at $z = 1.0$ mm because of weaker refraction. Consequently, for a fixed number of incident photons, the photon densities near the skin surface decrease in the water cases. When the surface roughness of the skin surface is doubled to $\delta_{01} = 0.4$ μm with water as the ambient medium, the peak at the focal point is decreased as expected, but still much higher than that of smoother surfaces with air as the ambient medium.

It is clear from Fig. 4 that the relative ratio of the peak to the background photon density at the focal spot is very sensitive to the index mismatch and the roughness at the skin surface. This further proves that the peak above the background in the photon density is due to the undisturbed photons in the converging laser beam. Therefore consideration of a converging beam provides a unique configuration to allow us to separate the photon density at the focal spot into two parts: a background that is due to the deflection at the two interfaces or scattering in bulk and a peak above the background that is due to the converging of the undisturbed photons.

To study the effect of roughness at the dermoepidermal junction, the index of the epidermis needs to be different from that of the dermis. With $n_1 = 1.45$, $n_2 = 1.41$, and $\delta_{12} = 10$ μm, the dermoepidermal junction is visible in the photon density plotted in the y–z plane in Fig. 5 for the presence of index mismatch. In this case the ambient medium is assumed to be water, and the rest of the parameters are kept the same as those in Fig. 3. The z dependence of the

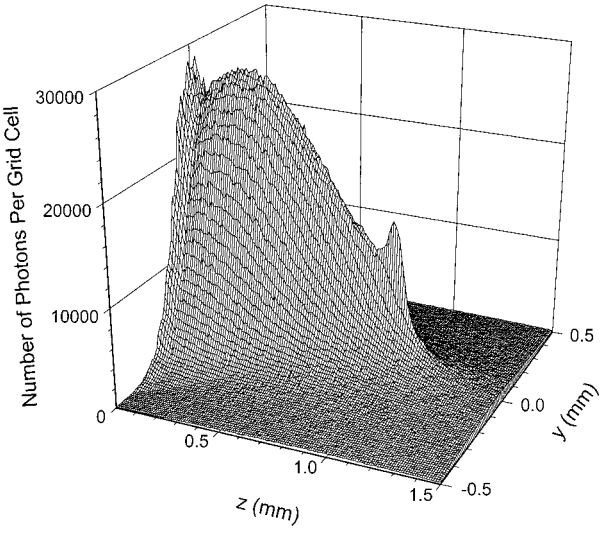

Fig. 5. Photon density in the y–z plane with water as the ambient medium ($n_0 = 1.33$) and $n_1 = 1.45$, $n_2 = 1.41$, and $\delta_{12} = 10$ μm. All other parameters are identical to those in Fig. 3.

photon density of this case is displayed in Fig. 6 on the z axis along with two other cases of different δ_{12}. Here we see a sharp division between the two layers at the junction that is due to the index mismatch and different bulk parameters. As the roughness at the junction increases by double δ_{12}, from 5 to 10 μm, the peak at the focal point decreases significantly because of strong deflection of the unattenuated photons at the junction. Also, when $\delta_{12} = 20$ μm, the peak formed by the undisturbed photons completely disappears.

The effect of the index mismatch at the dermoepidermal junction on the light distributions is illustrated in Fig. 7 with the refractive index of the dermis n_2 changed from 1.41 to 1.33 while that of the epidermis is kept constant at $n_1 = 1.41$. It is clear from

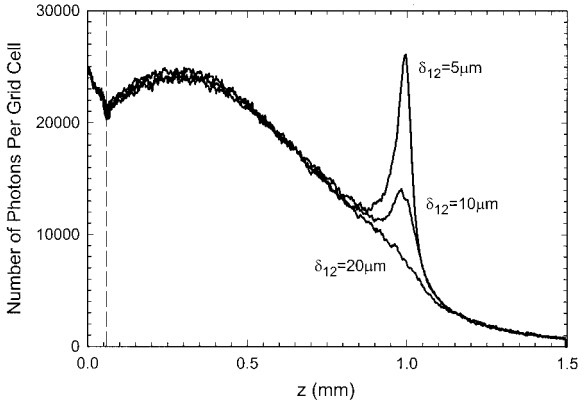

Fig. 6. Photon density z dependence on the z axis for three cases of different surface roughnesses at the dermoepidermal junction δ_{12}. All other parameters remain the same for the three cases: $n_0 = 1.33$, $n_1 = 1.45$, $a_{01} = 20$ μm, $\delta_{01} = 0.2$ μm, $\mu_{a1} = 5.0$ mm^{-1}, $\mu_{s1} = 10.0$ mm^{-1}, $g_1 = g_2 = 0.9$, $a_{12} = 80$ μm, $n_2 = 1.41$, $\mu_{a2} = 0.5$ mm^{-1}, and $\mu_{s2} = 5.0$ mm^{-1}. The dashed line indicates the position of the dermoepidermal junction.

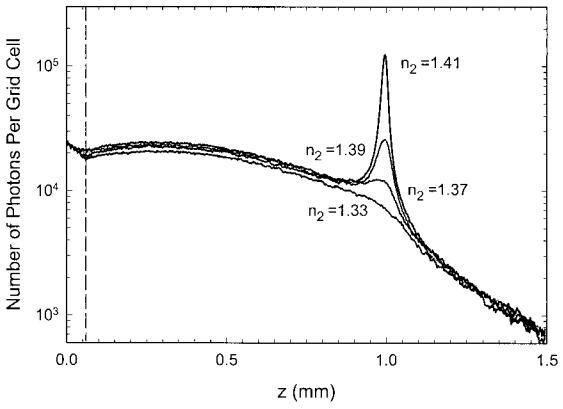

Fig. 7. Photon density z dependence on the z axis for four cases of different refractive indices of dermis n_2 with $n_1 = 1.41$ and $\delta_{12} = 10$ μm. All other parameters are identical to those in Fig. 5, and the dashed line indicates the position of the dermoepidermal junction.

these results that the increased index mismatch at the two rough interfaces enhances the effect of the rough surface. Furthermore, we note that the undisturbed portion of the incident light remains significant near the focal spot in comparison with the background scattering even in a strong turbid medium at an optical depth of $\mu_t z = 5.4$.

5. Discussion

The results of Monte Carlo simulation reported in this paper provide a quantitative analysis of the dependence of the light distribution in a two-layer skin tissue phantom on the interface roughness and index mismatch that is consistent with radiative transfer theory. Although radiative transfer theory has been widely accepted for treating light propagation in the bulk of turbid media, applications to the light interaction with rough interfaces have not been considered, to our best knowledge. On the basis of the degree of roughness in the cases considered in this paper, we have adopted an approach in which the rough interfaces are treated as locally flat. In these cases the light wavelength is sufficiently small compared with the transverse dimension of the fluctuation in surface height, and the photons can be described as packets of energy and effectively treated as plane wavelets; the Fresnel formula is used to determine the local reflectivity at the rough interfaces. This approach is similar to radiative transfer theory, in which the effect of bulk scattering, which is due to microscopic inhomogeneity in dielectric property, on light distribution is described by a scattering coefficient μ_s and a scattering phase function $p(\theta)$. In principle, the parameters μ_s and $p(\theta)$ can be derived on the basis of electromagnetic wave theory such as the Mie theory, which provides a foundation, albeit partially, for the phenomenological radiative transfer theory.[3] We note that our approach of treating light interaction with a rough interface does not provide phase information of the electromagnetic

field and fails to explain coherent phenomena such as the enhanced backscattering from rough surfaces.[19]

Three conclusions can be drawn from these simulation results. First, rough tissue interfaces can strongly affect the light distributions of a converging beam near the focal point, and a large index mismatch at these interfaces can significantly enhance such an effect. As is shown in Fig. 6, for an index mismatch of 0.04 at the dermoepidermal junction, the photon density ratio of the peak above the background to the background at the focal spot is reduced by a factor of 3.3 when the roughness parameters δ_{12} increase from 5 to 10 μm. This ratio decreases from 13.6 to 0.45 when the index mismatch at the junction increases from 0.00 to 0.02 (see Fig. 7). This photon density ratio is proportional to the ratio of two types of photon population near the focal point: the undisturbed photons and the scattered plus the deflected photons. Based on these results, it becomes clear that neglecting interface roughness can lead to a significant overestimation of the bulk scattering coefficient from measurements relying on separating the two types of photon outside a tissue sample, because the deflection of photons is implicitly included as a part of bulk scattering by assuming that the interfaces are smooth and flat.[23,24] The roughness of the tissue interfaces, however, has not been considered because of the lack of modeling tools and detailed knowledge of refractive indices of skin tissues. Further studies are in progress to investigate the overestimation of the scattering coefficient through transmittance and reflectance measurements of slab tissue samples that are due to rough interfaces. Second, our results indicate that the refractive index plays an important role in tissue optics involving rough interfaces for converging beams and illustrates the importance of accurate knowledge of the refractive index of biological tissues in the spectral region of interest. The measurement of the refractive index, however, remains an experimental challenge for turbid media such as biological tissues. One possible solution is to combine a spatial-filtering technique with immersion of the sample in a liquid of known refractive index. The index of the tissue sample can be determined when the undisturbed portion of the transmitted light is maximized with a clear liquid of known index that matches that of the tissue sample. Last, we point out that when treatment of skin lesion in the dermis layer is desired with a focused laser beam, it can be easily seen from our results that reducing the index mismatch at the skin surface can significantly increase the laser irradiance at the focal spot under the surface.

Some of the numerical simulations were performed on the Origin 2000 computers through an allocation grant from the North Carolina Supercomputing Center. This work was partly supported by the U.S. National Science Foundation under grant PHY-9973787 and the U.S. National Institutes of Health under grant R15GM/OD55940-01.

References

1. R. R. Anderson and J. A. Parrish, "The optics of human skin," J. Invest. Dermotol. **77,** 13–19 (1981).
2. M. J. C. van Gemert, S. L. Jacque, H. J. C. M. Sterenborg, and W. M. Star, "Skin optics," IEEE Trans. Biomed. Eng. **36,** 1146–1154 (1989).
3. A. Ishimaru, *Wave Propagation and Scattering in Random Media* (Academic, New York, 1978), Vol. 1.
4. B. C. Wilson and G. Adams, "A Monte Carlo model for the absorption and flux distributions of light in tissue," Med. Phys. **10,** 824–830 (1983).
5. M. Keijzer, S. T. Jacques, S. A. Prahl, and A. J. Welch, "Light distributions in artery tissue: Monte Carlo simulations for finite-diameter laser beams," Lasers Surg. Med. **9,** 148–154 (1989).
6. R. Marchesini, C. Clemente, E. Pignoli, and M. Brambilla, "Optical properties of *in vitro* epidermis and their possible relationship with optical properties of *in vivo* skin," J. Photochem. Photobiol. B **16,** 127–140 (1992).
7. R. Graaff, A. C. M. Dassel, M. H. Koelink, F. F. M. de Mul, J. G. Aarnoudse, and W. G. Zijlstra, "Optical properties of human dermis *in vitro* and *in vivo*," Appl. Opt. **32,** 435–447 (1993).
8. J. M. Schmitt, G. X. Zhou, and E. C. Walker, "Multilayer model of photon diffusion in skin," J. Opt. Soc. Am. A **7,** 2141–2153 (1990).
9. I. D. Miller and A. R. Veith, "Optical modelling of light distributions in skin tissue following laser irradiation," Lasers Surg. Med. **13,** 565–571 (1993).
10. W. Verkruysse, J. W. Pickering, J. F. Beek, M. Keijzer, and M. J. C. van Germert, "Modeling the effect of wavelength on the pulsed dye laser treatment of port wine stains," Appl. Opt. **32,** 393–398 (1993).
11. M. Rajadhyaksha, R. R. Anderson, and R. H. Webb, "Video-rate confocal scanning laser microscope for imaging human tissues *in vivo*," Appl. Opt. **38,** 2105–2115 (1999).
12. G. J. Tearney, M. E. Brezinski, J. F. Southern, B. E. Bouma, M. R. Hee, and J. G. Fujimoto, "Determination of the refractive index of highly scattering human tissue by optical coherence tomography," Opt. Lett. **21,** 2258–2260 (1995).
13. X. H. Hu, "Efficient use of *Q*-switched lasers in the treatment of cutaneous lesions," in *Lasers in Surgery: Advanced Characterization, Therapeutics, and Systems V*, by R. R. Anderson, ed., Proc. SPIE **2395,** 586–591 (1995).
14. Z. Song, K. Dong, X. H. Hu, and J. Q. Lu, "Monte Carlo simulation of converging laser beams propagating in biological tissue," Appl. Opt. **37,** 2944–2949 (1999).
15. H. G. Burkitt, B. Young, and J. W. Heath, *Wheater's Functional Histology*, 3rd ed. (Longman Group, Edinburgh, 1993), Chap. 9.
16. G. Plewig and T. Jansen, "Size and shape of corneocytes: variation with anatomic site and age," in *Bioengineering of the Skin: Skin Surface Imaging and Analysis*, by K.-P. Wilhelm, P. Elsner, E. Berardesca, and H. I. Maibach, eds. (CRC, Boca Raton, Fla., 1996), Chap. III-3.
17. C. el Gammal, A. M. Kligman, and S. el Gammal, "Anatomy of the skin surface," in *Bioengineering of the Skin: Skin Surface Imaging and Analysis*, by K.-P. Wilhelm, P. Elsner, E. Berardesca, and H. I. Mailbach, eds. (CRC, Boca Raton, Fla., 1996), Chap. I.
18. N. Garcia and E. Stoll, "Monte Carlo calculation for electromagnetic wave scattering from random rough surfaces," Phys. Rev. Lett. **52,** 1798–1801 (1984).
19. A. A. Maradudin, T. Michel, A. R. McGurn, and E. R. Mendez, "Enhanced backscattering of light from a random grating," Ann. Phys. **203,** 255–307 (1990).
20. P. Tran and A. A. Maradudin, "Scattering of a scalar beam from a two-dimensional randomly rough hard wall: enhanced backscattering," Phys. Rev. B **45,** 3936–3939 (1992).

21. P. Beckmann and A. Spizzichino, *The Scattering of Electromagnetic Waves from Rough Surfaces* (Pergamon, London, 1963), Chap. 3.
22. J. Q. Lu, A. A. Maradudin, and T. Michel, "Enhanced backscattering from a rough dielectric film on a reflecting substrate," J. Opt. Soc. Am. B **8,** 311–317 (1991).
23. V. G. Peters, D. R. Wyman, M. S. Patterson, and G. L. Frank, "Optical properties of normal and diseased human breast tissues in the visible and near infrared," Phys. Med. Biol. **35,** 1317–1334 (1990).
24. Y. Du, M. Cariveau, G. W. Kalmus, J. Q. Lu, and X. H. Hu, "Experimental study of optical properties of porcine skin dermis from 900 to 1500 nm," in *Optical Biopsy III*, R. R. Alfano, ed., Proc. SPIE **3917,** 184–192 (2000).